On the use of Principal Component Analysis in analysing Cepheid light curves

S. M. Kanbur D. Iono, [1]★ N. R. Tanvir,[2] M. A. Hendry,[3]

[1] *Department of Astronomy, University of Massachusetts, Amherst, MA 01003*

[2] *Department of Physical Science, University of Hertfordshire, College Lane, Hatfield, AL10 9AB, UK*

[3] *Department of Physics and Astronomy, University of Glasgow, Glasgow, UK*

1 February 2008

ABSTRACT

We show how Principal Component Analysis can be used to analyse the structure of Cepheid light curves. This method is more efficient than Fourier analysis at bringing out changes in light curve shape as a function of period. Using this technique, we study the shape of fundamental and first overtone mode Cepheid light curves in the Galaxy, LMC and SMC over a wide period range. For fundamentals, we find evidence for structural changes at $\log P \approx 1.55, 2.1$. It is suggested that the feature at $\log P \approx 2.1$ is associated with a resonance in the Cepheid normal mode spectrum. For overtones, we recover the Z shape in the R_{21} period plane and reproduce the metallicity dependence of this Z shape.

Key words: Principal Component Analysis, Cepheids

1 INTRODUCTION

Cepheids play a vital role in astrophysics. Their pulsational properties pose constraints that stellar pulsation and evolution theories must satisfy simultaneously. Further they are the keystone of the extra-galactic distance scale through the period – luminosity (PL) relation. In this paper, we describe a new way of analysing the structure of variable star light and velocity curves, Principal Component Analysis (PCA). The technique is more general and more efficient at describing structure than Fourier analysis (Hendry et al 1999, Kanbur et al 2000a), Tanvir et al 2000). Hendry et al 1999 also analyzed the period-luminosity-light curve shape relation for Cepheids in the Galaxy and LMC. This was extended to the SMC by Ligeza and Schwarzenberg-Czerny (2000).

In this paper we use PCA to examine light curve structure to search for other resonances which have been claimed in the literature (Antonello 1998). We identify two features in the light curve structure of long period Cepheids at $\log P \approx 1.55, 2.1$ days. The feature at $\log P \approx 2.1$ may be connected with resonances in the Cepheid normal mode spectrum. The templates generated with PCA have also been used, together with Fourier decomposition, to fit sparse and noisy data to obtain good period and magnitude estimates (Tanvir et al 1999, Kanbur et al 2001).

Section 2 describes Fourier analysis as applied to variable star data and section 3 summarizes PCA. Sections 4 and 5 present our results using this method. Section 6 presents our conclusions and discussion and suggestions for further work.

2   PREVIOUS WORK

The technique of Fourier decomposition has been used for some time to analyse variable star data (Schaltenbrand and Tammann, 1971). In the seventies the method was revived by Simon and Lee (1981) who fitted expressions of the form,

$$A_0 + \sum_{k=1}^{k=N} (A_k cos(k\omega t + \phi_k)) \tag{1}$$

to observed data. They plotted the relative Fourier parameters,

$$R_{k1} = A_k/A_1, \phi_{k1} = \phi_k - k\phi_1 \tag{2}$$

describing light curve structure against period. These authors noted sharp breaks in the progression of ϕ_{k1} and R_{k1} against period at a period of 10 days. This was associated with the Hertzsprung progression, where a bump on the descending branch of short period ($P < 10$ days) Cepheids moves to the ascending branch of long period ($P > 10$ days) Cepheids. Using linear adiabatic models, Simon and Schmidt (1976) and Simon and Lee (1981) interpreted the Hertzsprung progression and the sharp break in the Fourier parameter plots at 10 days as evidence of a resonance between the fundamental mode, P_0, and the second overtone, P_2, such that $P_2/P_0 = 0.5$ at $P_0 = 10$ days. Since then, Fourier decomposition has been used to identify possible resonances in first and second overtone Cepheids (Antonello and Aikawa 1995, Antonello and Kanbur 1998). Microlensing surveys (MACHO, OGLE and EROS) have also made significant use of Fourier analysis (Welch et al. 1996, Beaulieu and Sasselov 1996, Udalski et al. 1999). Recently, Antonello and Morelli (1996) and Antonello (1998) suggested the presence of resonances in the normal mode spectrum of long period

Cepheids, namely $P_0/P_1 = 3/2$ at $1.34 < \log P_0 < 1.40$ days, $P_0/P_3 = 3$ at $1.40 < \log P_0 < 1.43$ days and $P_1/P_0 = 0.5$ at $1.95 < \log P_0 < 2.13$ days. Their argument was based on a Fourier analysis of observed light and velocity curves. Figure 1 is taken from Antonello and Morelli (1996) and shows a plot of the Fourier parameters R_{21} and ϕ_{21} plotted against period. Though it may be argued that there are breaks in this plot at periods around 20-25 ($\log P = 1.3$ to $\log P = 1.4$) days (see also figures 1 and 2 of Antonello and Morelli 1996), definitive conclusions are hard to draw. Figure 2 of Antonello (1998) extends the period range to about 150 days and was used by Antonello and co-workers to suggest the presence of a resonance at a period between 90 and 134 days.

3 PRINCIPAL COMPONENT ANALYSIS

Kanbur et al (2000a)), Hendry et al 1999 suggested the possibility of using the technique of Principal Component Analysis (PCA) in studying variable star data. Here we review and extend the formalism briefly described in Kanbur et al (2000a)). Let X_{ij} be the jth ($1 \leq j \leq P$) observed point on the ith ($1 \leq i \leq N$) light curve. The input matrix of the data is

$$S_{jk} = \frac{1}{N} \sum_{i=1}^{i=N} X_{ji} X_{ki}, \tag{3}$$

sometimes referred to as the covariance-variance matrix (Murtagh and Heck 1987). This measures the relationship between the jth and k^{th} points, averaged over all N stars in the sample. In our use of PCA, we seek to write any Cepheid light curve as a linear combination of elementary light curves, u_i^t,

$$V(i) = \sum_{t=1}^{t=P} PC_t(i) u_i^t. \tag{4}$$

Here, $PC_t(i)$ are Principal Component coefficients so that $PC1$ for star i is $PC_1(1)$ etc. One example of such elementary light curves are the harmonics in equation (1). Given the assumption that the elementary light curves are harmonics, then fitting a Fourier expansion to variable star data will find the best coefficients $PC_t(i)$ in a least squares sense. That is, a Fourier fit will yield estimates for A_k and ϕ_k in equation (1) that minimize the sum of squared deviations in magnitude between the model and the observed data. The technique of PCA will optimise, in a least squares sense, the fit of the data to the model of equation (4) without any prior assumption about the nature of the functions u_i^t (Murtagh and Heck 1987); instead the u_i^t and their coefficients are determined entirely by the properties of the input matrix, S. Further the functions u_i^t are orthogonal to each other and hence the elementary light curves in (4) are distinct from each other. It can be shown that this optimal set of curves,

$\{u^t\}$, is given by the solution of the eigenvalue equation,

$$Su = \lambda u. \tag{4}$$

Solution of this equation yields u_i^t and a λ^t for each vector u_i^t. After suitable normalization, the λ^t can be interpreted as the percentage variance in the light curve data explained by the tth light curve. We can project each light curve onto the eigenvectors $\{u_i^t\}, t = 1, ..., P$, by forming the sum,

$$PC_t(i) = \sum_{j=1}^{j=P} X_{ji} u_j^t. \tag{5}$$

Each Cepheid light curve $V(i), i = 1, .., N$ can then be represented as

$$V(i) = \sum_{t=1}^{t=P} PC_t(i) u_i^t. \tag{6}$$

In this work, we convert the Fourier expansion given in equation (1) to the equivalent form,

$$A_0 + \sum_{k=1}^{k=N} (a_k cos(k\omega t) + b_k sin(k\omega t)), \tag{7}$$

where,

$$A_k^2 = a_k^2 + b_k^2, tan(\phi_k) = b_k/a_k, \tag{8}$$

so that the X matrix consists of

$$X_{ij} = a_{ij}, X_{ij+1} = b_{ij}.$$

Therefore the resulting eigenvectors obtained from solving equation (4), that is the optimal basis set, are in fact a set of vectors consisting of a, b coefficients so that equation (6) becomes,

$$V(i) = \sum_{j=1}^{j=P} PC_j(i) (\sum_{k=1}^{k=P} (x_k^j cos(k\omega t) + y_k^j sin(k\omega t))). \tag{9}$$

In this equation, the x_k^j, y_k^j are fixed and obtained from the PCA analysis by the solution of equation (4). We can find a relation between Fourier coefficients and PCA coefficients, $PC_j(i)$, by equating $cos(k\omega t), sin(k\omega t)$ coefficients between equation (9) and (1). This yields,

$$A_k^2 = \left(\sum_{j=1}^{j=P} PC_j x_j^k \right)^2 + \left(\sum_{j=1}^{j=P} PC_j y_j^k \right)^2 . \tag{10}$$

$$tan(\phi_k) = -\frac{\sum_{j=1}^{j=P} (PC_j y_k^j)}{\sum_{j=1}^{j=P} (PC_j x_k^j)}. \tag{11}$$

This establishes a *direct* correspondence between the PC coefficients and the Fourier parameters which are plotted against period. In particular at the 10 day resonance, $R_{21} = A_2/A_1$ goes down. Plotting A_1, A_2 against period it is easy to see that this is because A_2 goes down at 10 days. If A_2 goes down then equation (10) implies that either PC_1 goes down or PC_2 goes down or

both go down. This proves that if there is a change in the structure of the light curve as shown by a change in the Fourier parameters, equations (10) and (11) guarantee that such a change will be reflected in the PC coefficients. It would be interesting to apply the amplitude equation formalism developed by Buchler (1993) to understand the physical nature of the PCA coefficients perhaps through the use of equations (10) and (11). Our initial work suggests that the $PC1$ coefficient is correlated with amplitude. We intend to pursue this, coupled with a PCA study of hydrodynamic model light and velocity curves in future work.

In a practical sense, the principal advantage of PCA is efficiency. PCA requires 4 to 6 parameters to describe Cepheid light curve structure (including bump Cepheids, Kanbur et al 2000a)) whereas an 8th Fourier fit needs 16 parameters. It is true that A_1, R_{21} and ϕ_{21} - that is three Fourier parameters are often used in comparing models and observations but in order to get stable values of these coefficients, a 6 to 8 order Fourier fit is needed.

We can plot the $PC_t(i)$ against period analogously to the way Fourier parameters in equation (2) are plotted against period. Recall that figure 1 shows a plot of the Fourier parameters R_{21} and ϕ_{21} plotted against period for the Cepheid data presented in Antonello and Morelli (1996). The upper panel, which shows ϕ_{21} against log period, indicates clearly a discontinuity at $\log P = 1$ but little structure thereafter. The lower panel, which shows R_{21} against log period also exhibits clear structure at $\log P \approx 1$, followed by a general rise to $\log P \approx 1.4$ and some scatter thereafter. It should be noted that Antonello (1998) included more data on longer period Cepheids and found some evidence of a decrease at large ($\log P \approx 2$) in the R_{21} - period plane.

For our PCA analyses, we used V band data from the Galaxy, LMC and SMC published by Moffett and Barnes (1989) and Berdnikov and Taylor (1995), and Antonello (1998) to carry out such a procedure. We emphasize that all this data has *good* Fourier decomposition such that the light curve obtained from the Fourier decomposition is an excellent representation of the actual data points with few numerical bumps or wiggles. The top and bottom panel of figure 2 shows plots of $PC_1(i)$ and $PC_2(i)$ against the logarithm of the period (see equation 5). Open circles denote Galactic Cepheids, solid circles and open stars are the LMC and SMC respectively. The data used were taken from the McMaster web site. Typical error bars (see section 4) are shown in the top left hand corner of the upper panel. This error bar is applicable to all subsequent plots of the PC coefficients. Taken together, these first two principal components account for 97 percent of the variation in the data.

The top panel, showing the first principal component, PC1, plotted against the logarithm of the period displays some scatter for $\log P$ less than one, an abrupt decrease at $\log P \approx 1$ and then a rise from $\log P = 1$ to $\log P = 1.2$. There is a "plateau" till about $\log P = 1.55$, after which PC1 falls gradually till $\log P = 2.1$. The bottom panel, which shows the second principal component, PC2, shows a similar pattern to the top panel, but with significantly smaller scatter. In particular the break and sharp decrease at $\log P = 1$ is very clean, the general rise from $\log P = 1$ to $\log P = 1.55$ has little scatter. There is a sharp turnover at $\log P = 1.55$ and a decline to a minimum at $\log P = 2.1$. We notice that PC1 is always positive while PC2 can be either positive or negative. This is because each light curve is written as equation (6), with the first term in this sum, $PC_1(i).u_1(i)$, being the basic light curve, while the second term, $PC_2(i).u_2(i)$ is a second order term showing corrections to the basic light curve. It can be argued that features like bumps are second order effects and should be more evident in the second and higher principal components.

Equation (10) and the shape of the plots in figure 2 enables us to categorically state that we see the presence of the resonance at $\log P = 1$ in the PC plots. The bottom panel shows a sharp drop at $\log P = 1$ followed by a gradual rise in PC2 from $\log P = 1$ to $\log P = 1.55$ and a gradual decline thereafter till $\log P = 2.1$. In both panels, we see three stars with PC1, PC2 values significantly lower than normal at $\log P \approx 1.6 - 1.7$, and one star with a significantly higher than normal value at $\log P \approx 1.8$. We do not treat these stars here but note that our error analysis, described in the next section, suggests that the uncertainties on the PC1/PC2 values are small. Despite this, figure 2 clearly shows a definite maximum at $\log P = 1.55$ and a well defined decrease thereafter till $\log P = 2.1$. This latter minimum is dependent on 4 stars. The data for these stars is exactly as used by Antonello and Morelli (1996), and Antonello (1998) with sufficient phase coverage to permit an excellent Fourier decomposition. We suggest that this rise and fall in the PC1/PC2 values is real and caused by pulsation physics. We believe that figure 2 and constitutes convincing evidence that the change in the structure of light curve shape at $\log P = 2.1$ is very similar to that at $\log P = 1$. Since a resonance is associated with the latter, it is our contention that the feature at $\log P = 2.1$ is associated with a resonance in the Cepheid normal mode spectrum. This has already been suggested by Antonello and Morelli (1996) using Fourier decomposition as in figure 1 as evidence. We feel that our figure 2 comprises a much stronger case than has hitherto been presented. One caveat with this is that changes in light curve shape are not necessarily associated with resonances (Kienzle et al, 1999).

4 ERROR ANALYSIS

PCA has the nice property that if the data are normally distributed, then

$$\sigma^2(PC_t(i)) = \sum_{j=1}^{j=P} (\sigma^2(X_{ij})u_j^t. \tag{6}$$

X_{ij} is the jth observed point on the ith star. However, with the specification that phase 0 is maximum light, we have chosen to parameterize the light curves by the Fourier expansion,

$$A_0 + \sum_{k=1}^{k=P} [a_k cos(k\omega t) + b_k sin(k\omega t)], \tag{7}$$

which is entirely equivalent to equation (1). Now our X matrix consists of

$$X_{ij} = a_{ij}, X_{ij+1} = b_{ij},$$

where the a_{ij}, b_{ij} are the a_j, b_j in expression (7) for star i. This can be viewed as an initial guess. The PCA approach uses this to find the "optimal" way to represent light curves via equation (4). Consequently, the quality of the Fourier decomposition used has a bearing on the conclusions of this paper. As stated previously, the Fourier decompositions used were those carried out by the original authors of the data used. Superimposing the light curve produced by the Fourier decomposition on the original data points yielded an excellent match with no numerical bumps or wiggles in the Fourier decomposition light curve. Hence in our application of PCA, we require good enough phase coverage to permit a reasonable Fourier decomposition. Given this situation, it is our thesis that PCA is more efficient at bringing out significant changes in light curve shape.

In obtaining the fit given in (7) to the actual data, we can write the problem as

$$\underline{V} = \underline{A}\underline{\beta},$$

where $\underline{V}$ is the vector of data, the observed magnitudes, $\underline{A}$ is a known matrix and $\underline{\beta}$ is the vector of unknowns, consisting of the a_k, b_k in equation (7). A least squares estimate $\hat{\beta}$, for β can then be obtained. If the photometric errors are normally distributed, as is normally the case,

$$\underline{V} = \underline{A}\underline{\beta} + \underline{\epsilon}$$

where,

$$\epsilon \sim N(\underline{V}, \sigma^2),$$

then it can be shown that $\hat{\underline{\beta}}$ is normally distributed. Since the $\hat{\underline{\beta}}$ consist of the a_{ij}, b_{ij}, which make up the input matrix to the PCA, our input data is normally distributed and hence equation (6) applies. Moreover, $\sigma^2(X_{ij})$ is obtained eas-

ily via standard numerical techniques like Singular Value Decomposition. This enables a complete estimate of the error on $PC_t(i)$ which is the quantity considered in this paper. If the phase coverage is good, then the formulae given by Petersen (1986) can be used as an accurate estimate of $\sigma^2(X_{ij})$.

Figure 3 shows the bottom panel of figure 2 but with error estimates derived using the Petersen (1986) formulae. The larger error bars near $\log P = 1.5$ are due to a poorer Fourier fit since bad fits are reflected in the large standard deviation of the Fourier fit and the subsequent large error in the Principal Component diagrams. It can also be the case that numerical wiggles are present in the Fourier fit despite a small standard deviation. This was not the case with the data used in this study. In any case, such "wiggles" would be contained in the higher order Fourier parameters and hence in the higher order principal components. Nevertheless the figure clearly shows that the structure of figure 2 is real. Further these error bars are not significantly altered if photometric errors associated with the data are included in the error analysis.

5   ASYMMETRY PARAMETER

Antonello (1993) used the asymmetry parameter, defined as $(M - m)$, where M and m are the phase of maximum and minimum light respectively. Using the same data as shown figure 1, we plot $1 - (M - m)$ against log period in figure 4. Again we see that at 10 days, a sharp change occurs in this asymmetry parameter. On either side of the resonance, minimum light occurs at a phase of about 0.7, while at the resonance it occurs at a phase of 0.5. The light curve shape near the resonance becomes more sinusoidal, departing from the usual saw tooth shape. While this behavior deserves further investigation, in the context of the present paper, we note that there is a similar change in the asymmetry parameter at $\log P \approx 2.1$. The feature at $\log P \approx 1.55$ is the reverse of what happens at a resonance - the phase of minimum light occurs even later than usual and the light curves take on a more saw tooth like appearance. We comment on this later and suggest figure 3 as further evidence of a resonance at $\log P = 2.1$.

6   I BAND DATA

We performed the PCA analysis on I band data Cepheid data again from Moffett and Barnes (1989), and Berdnikov and Turner (1995). Note that this was the same data as for our V band analysis without the extra long period stars

studied in Antonello (1998). Figure 5 shows the first two principal components from the I band data. They are generally similar to the V band figures. The points form a clump for stars with periods smaller that $\log P = 1$. At $\log P = 1$, there is a sharp discontinuity to negative values of PC1/PC2. From $\log P = 1$, PC1 gradually rises to a peak at about $\log P = 1.6$. After this PC1/PC2 fall again to negative values at $\log P = 2.1$. Since there are theoretically expected differences in a Cepheids light curve as the wavelength changes, we would expect some differences but the fact that the general structure is the same indicates strongly that PCA is a bona fide technique in analysing variable star light curve structure.

In this study, we performed the PCA of V and I band data separately but there is no reason why the V and I band data cannot be analysed jointly. In fact such an approach could lead to insights into structural changes across period and wavelength. We leave a detailed comparison of the V/I band PCA analysis to a future paper.

7   EROS DATA

EROS (Beaulieu et al. 1995,) is a microlensing search that has resulted in Cepheid light curves for some 550 fundamental and first overtone Cepheids in the LMC and SMC. Figure 6 and 7 shows plots of the first two principal components plotted against period. These data were kindly provided by Beaulieu (2000, private communication). The open and dark circles represent fundamental and first overtone oscillators respectively. We see a clear differentiation between the two types in both components. Figures 8 and 9 show the first two principal components plotted against period for fundamental mode Cepheids from the SMC and LMC. Open and dark circles represent the LMC and SMC respectively. We see clearly the position of the resonance at $\log P = 1$, confirming with another data set that PCA can pick up the presence of this resonance. We note that at given period, there is considerable scatter. Using our error analysis techniques, it can be shown that the error bars on these points are considerably less than the scatter at a given period. Hence this scatter is real and presumably caused by differences in global stellar parameters leading to differences in light curve structure. The SMC stars extend to shorter period and there is a tendency for shorter period stars to have higher values of PC2/PC1.

8   OVERTONES

It is well known that first overtone Cepheids show a change in the shape of the first overtone light curve at 3.2, 2.7 and 2.2 days for the Galaxy, LMC and SMC respectively (Beaulieu, private communication). To investigate how the PCA technique works in this regard, we present in figures 10-12 plots of the PC coefficients for Galactic, LMC and SMC first overtone stars. Figure 10 uses Galactic overtone data taken from Antonello and Poretti (1986). No discernible pattern is visible here, perhaps due to the relatively few data points. Figure 11 shows the the first two PC components for the EROS data with the LMC and SMC represented by open and solid circles respectively. There is significant structure but no definitive conclusions can be made about changes in structure at periods close to 3.2 and 2.7 days. Because of this, we also analyzed the OGLE survey data (Udalski et al 1999) which has detected about 500 and 800 overtones in the LMC and SMC respectively. Figure 12 shows the first two principal components for the LMC and SMC using OGLE first overtone data. If we initially look at the PC2 plot, for periods greater than about $\log P \approx 0$, we see an increase in PC2 with period to a maximum followed by a decline. The maximum for the LMC and SMC is at $\log P \approx 0.5$ and $\log P \approx 0.4$ respectively. These periods correspond closely to the periods at which changes in the structure of plots of R_{21} against period are seen for overtone light curves in the LMC and SMC (Udalski et al 1999). There is considerable structure in figure 12 which will be treated in a future paper but the main point for the purposes of this study is that the PCA approach picks out changes in the structure of overtone light curves as a function of metallicity.

9   DISCUSSION

We have developed a new way of analysing the structure of Cepheid light curves, Principal Component Analysis, which is much more efficient at bringing out changes in light curve structure than Fourier analysis. The method is particularly suitable to analyse the vast quantity of light curves produced by the MACHO, EROS and OGLE projects. We emphasize that our comparison between PCA and Fourier analysis is made only for those situations when a reliable Fourier decomposition already exists. In this case, PCA can be used to reproduce the light curve with about half the parameters needed by the Fourier decomposition technique. We have shown that PCA is a powerful method with which to detect changes in light curve shape. Since light curve shape changes can be associated with the resonances, PCA will be a powerful tool to search

for resonances in observed Cepheid light *and* velocity curves since there is no reason why this technique cannot be applied to velocity curves. The reliable detection of resonances is important because this can be used to place important constraints on global stellar parameters such as the mass, luminosity, effective temperature and metallicity (Simon and Kanbur 1994).

Specifically, we have found that based on a PCA analysis of Cepheid light curves and an examination of the asymmetry parameter, the structure of Cepheid light curves exhibit similar features at $\log P = 1$ and $\log P = 2.1$ in the following sense: at both periods, the phase at minimum light is close to 0.5 and the $PC1$, $PC2$ coefficients attain local minima. The approach to these local minima is different in the two cases but nevertheless there is a local minima at both periods. This clearly suggests a significant change in the shape of the light curve at these two periods. Since equations (10 and 11) establish a direct link between Fourier parameters and PC coefficients, this also implies a change in the Fourier parameters at these periods. Indeed figure 2 of Antonello (1988) has shown some evidence that the ratio R_{21} goes down at $\log P \approx 2.1$. We suggest that our results strengthen the case for an important change in the light curve shape at $\log P \approx 2.1$. Model calculations are needed to confirm if a resonance is indeed present and is associated with the fundamental and first overtones $P_1/P_0 = 0.5$ as suggested by Antonello (1988). Another feature present in the PCA and asymmetry plots is the maximum at $\log P = 1.55$. At this period, the light curves become less symmetric and the PC2 coefficient reaches its largest value. We note that Udalski et al (1999) show a plot of R_{21} against period for SMC Cepheids which also suggests a similar break at $\log P = 1.55$ though the number of stars with periods longer than $\log P = 1.55$ in their sample is too small to be definitive. Based on our PC2 plots, we conclude that this change in light curve shape is real and plan to investigate its cause. One possible way to sharpen this is to study light curve structure for long period ($\log P > 1$) Cepheids and examine the spread at given period as a function of other stellar parameters such as mean color. These topics will be the subject of a future paper.

Obviously more short period ($\log P < 1.7$) have been observed than long period ($\log P > 1.7$) Cepheids. This is caused both by the fact that it is difficult to obtain adequate phase coverage, sufficient for Fourier decomposition, for such long period stars, and possibly also because such long period stars may be intrinsically rare. However, the possible rarity of such stars does not affect the suggestion that a resonance occurs in the normal mode Cepheid spectrum at long periods. Since Cepheids in low metallicity environments will have higher
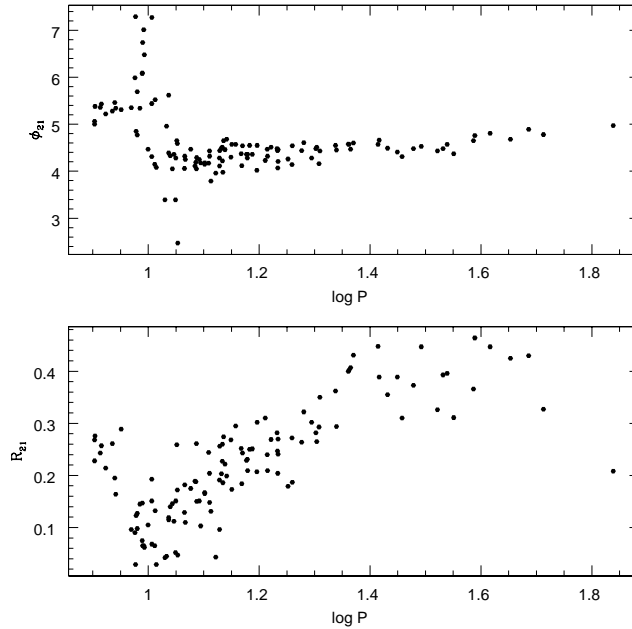
Figure 1. Plot of Fourier parameters against Period for long period Cepheids.

luminosities and hence longer periods for the same mass, the best chance to observe such stars is in low metallicity galaxies like the SMC. In fact the majority of the long period Cepheids used in this study were from the LMC/SMC.

Antonello and Morelli (1996) also suggested resonances in the period range $1.38 < \log P < 1.43$. Our analysis of the first two principal components (PC1/PC2) does not show any features in this period range. It is possible that these features may be visible in the higher order principal components and we leave this for future work. We also intend to apply PCA to the analysis of first overtone light and velocity curves. The greater efficiency of the method described here should enable a decisive contribution to answering where, if any, the resonance occurs ($P_4/P_1 = 0.5$ at $P_1 = 3.2$ days (Antonello and Poretti (1986), or $P_4/P_1 = 0.5$ at $P_1 = 4.58$ days (Kienzle et al 1999).

10   ACKNOWLEDGEMENTS

REFERENCES

Antonello E., 1990, Astr. and Astrophys., 180, 129

Antonello E., 1993, Astr. and Astrophys., 279, 125

Antonello E., and Aikawa, T., 1995 Astr. and Astrophys., 302, 105

Antonello E., and Morelli, E., 1996, Astr. and Astrophys., 314, 541
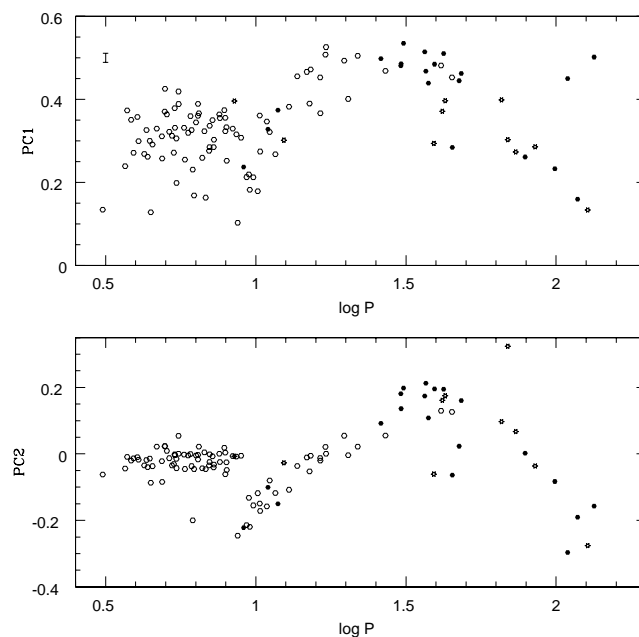
Figure 2. The first two Principal Components against log period. Open circles, galaxy, solid circles, LMC, open stars, SMC. Typical error bar plotted in top left hand side.
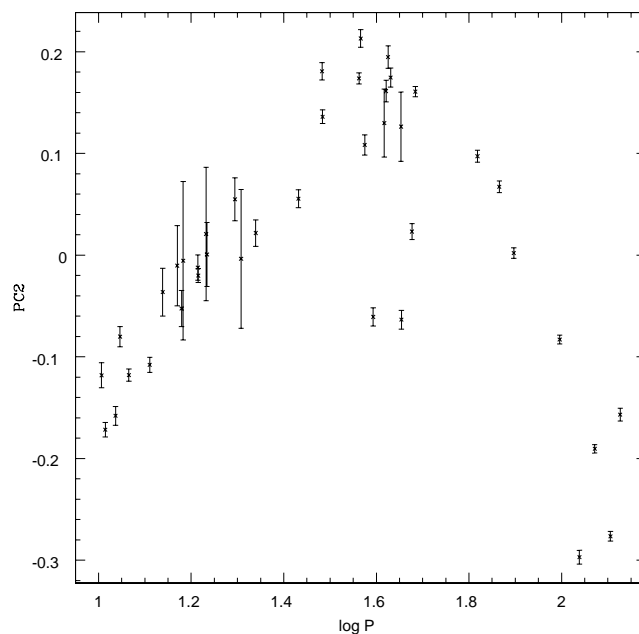
**Figure 3.** Errors associated with the second Principal Component plot

Antonello E., and Kanbur, S. M., 1997, MNRAS 286L, 33

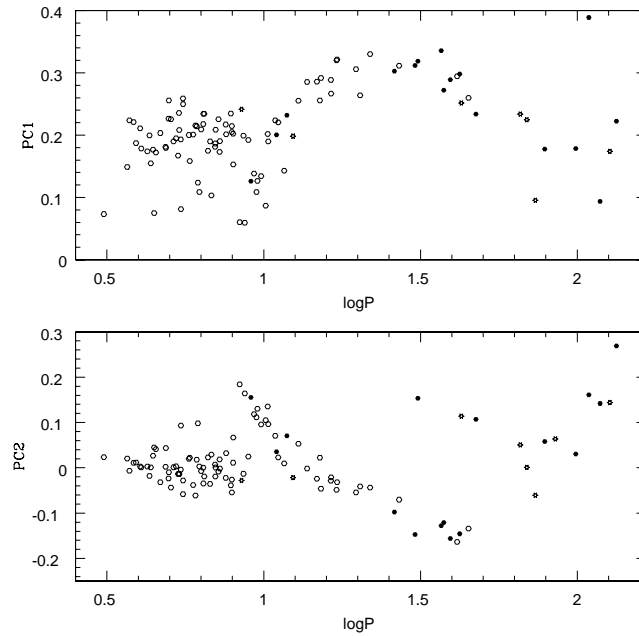Antonello E., 1998, Astr. and Astrophys., 333, L35

Beaulieu, J. P. & Sasselov, D., 1996, in "Variable Stars and the astrophysical returns of microlensing surveys", eds. Ferlet, Maillard, Raban, Editions Frontieres

Beaulieu, J. P., private communication

Berdnikov, L. N., & Turner, D. G. 1995, Astron. Lett., 21, 717
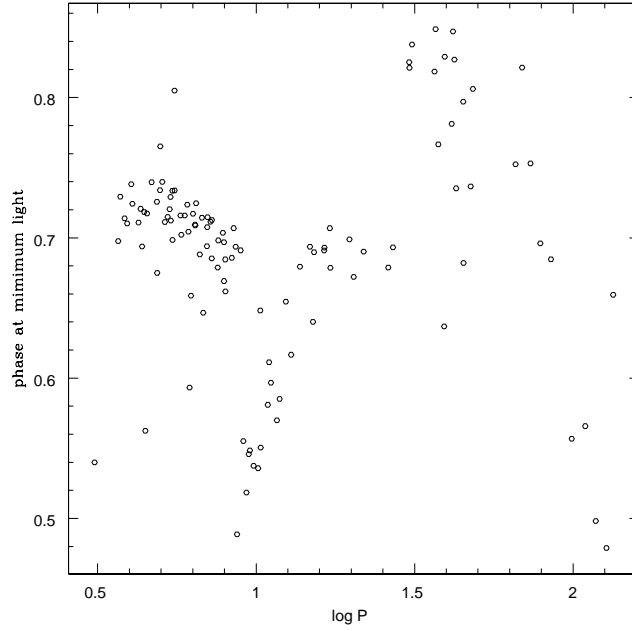
Figure 4. Phase of Minimum Light against Period

Figure 5. First two Principal Components plotted against period for I band Cepheid light curves

Hendry, M. A., Tanvir, N. R., Kanbur, S. M., 1999, ASP Conf. Series, 167, p. 192

Kanbur, S. M., Iono, D., Tanvir, N. Hendry, M., 2000a), ASP Conf. Series, 203, 56

Kienzle, F., Moskalik, P., Bersier, D., Pont, F., 1999, Astr. and Astrophys., 341 818

Ligeza, P. & Schwarzenberg-Czerny, A., 2000 in IAU Symposium no. 201

Moffett, T. J., & Barnes, T. G. 1984, APJS, 55, 389

Murtagh, F. and Heck, A., 1987, D. Reidel Publishing Company
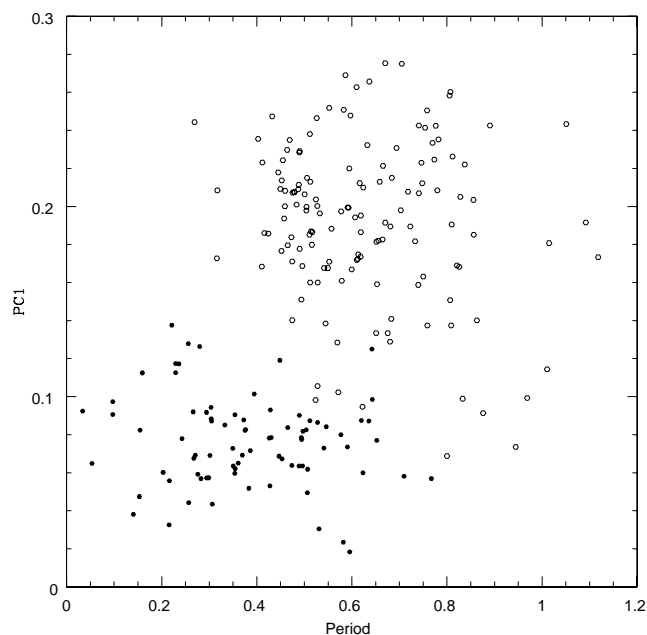
Figure 6. First Principal Component for LMC fundamental and first overtone Cepheids from EROS
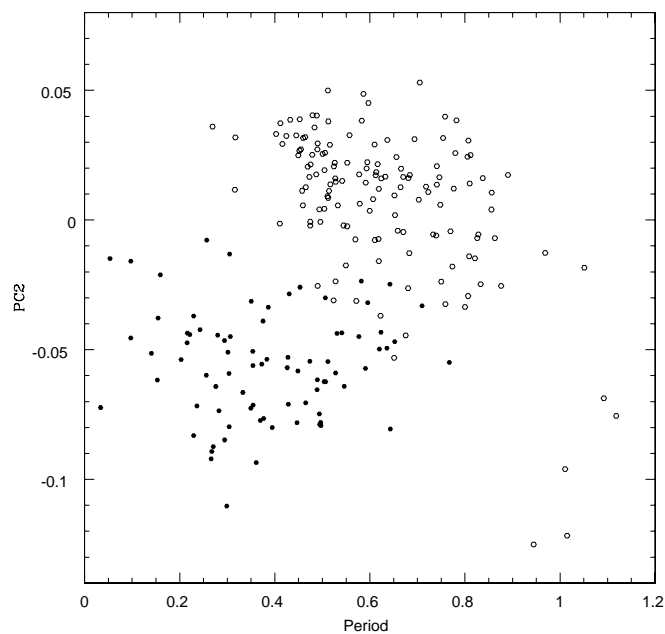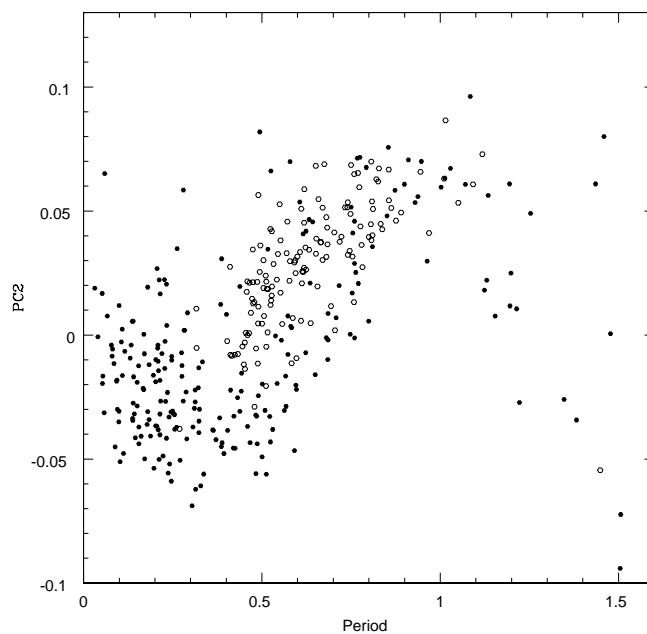

Figure 7. Second Principal Component for LMC fundamental and first overtone Cepheids from EROS

Petersen, J. O., 1986 Astr. and Astrophys., 170, 59

Schaltenbrand, R. and Tammann, G. A., 1971 Astr. and Astrophys. Suppl, 4, 265

Simon, N. R., and Schmidt, E. G. 1976, APJ, 189, 162

Simon, N. R., and Lee, A. S. 1981, APJ, 248, 291

Simon, N. R., and Kanbur, S. M. 1995, APJ 451, 703

Tanvir, N. R., Kanbur, S. M., Hendry, M. A., (2000),in preparation
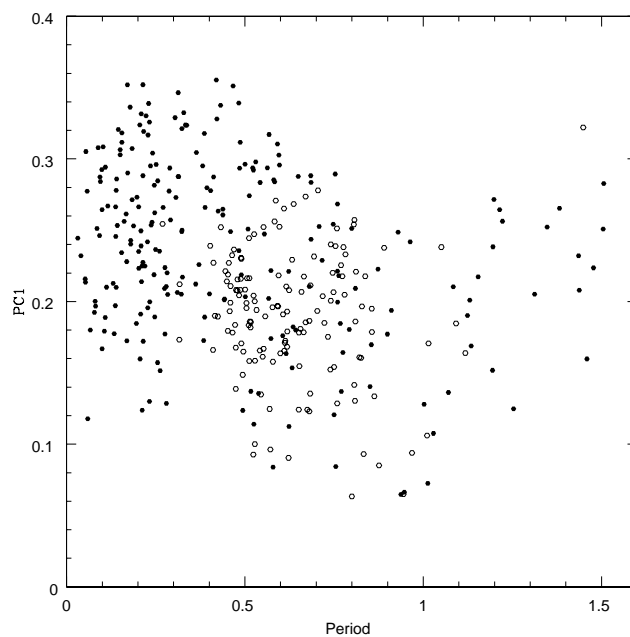
Figure 8. First Principal Component for LMC and SMC fundamental mode Cepheids from EROS
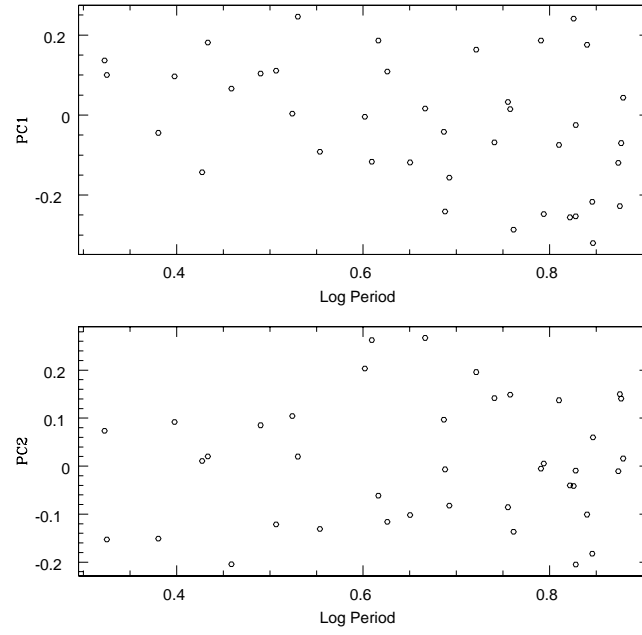

Figure 9. Second Principal Component for LMC and SMC fundamental mode Cepheids from EROS
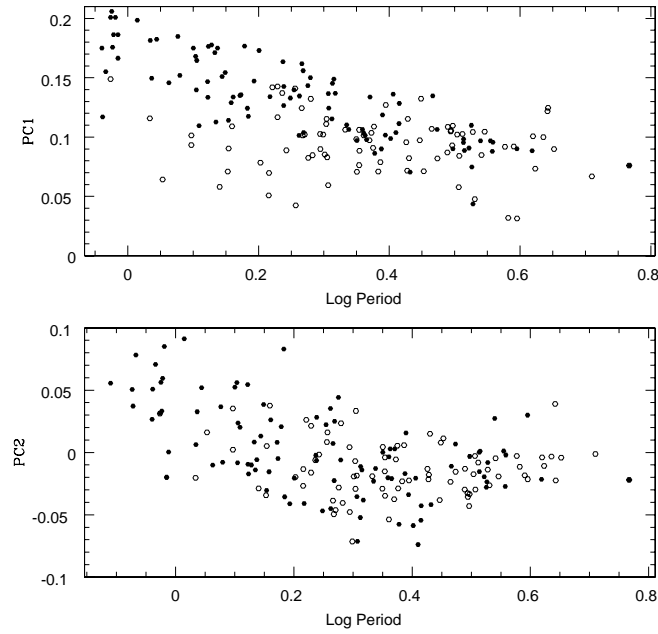
Udalski, A. et al, astro-ph 9912096

Welch, D et al., 1996 in "Variable Stars and the astrophysical returns of microlensing surveys",
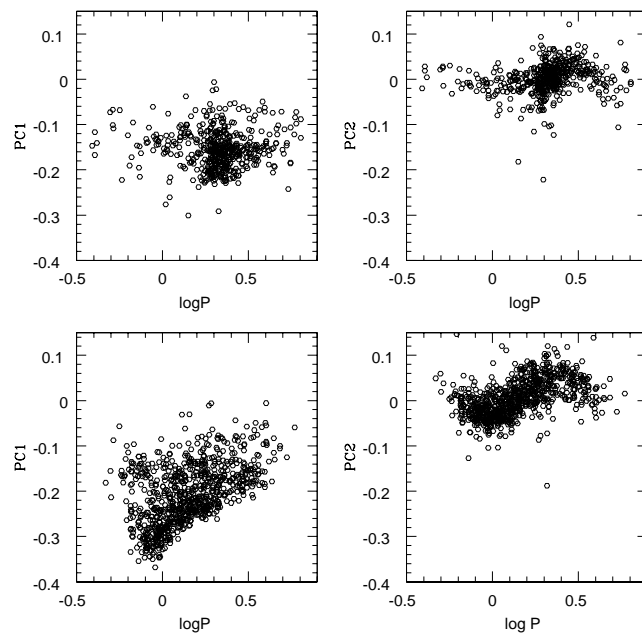
eds. Ferlet, Maillard, Raban, Editions Frontieres.

Figure 10. First two Principal Components for Galactic first overtone Cepheids

Figure 11. First two Principal Components for LMC and SMC first overtones. Open and solid circles are the LMC and SMC respectively

Figure 12. First two Principal Components for OGLE data for the LMC (top panel) and SMC (bottom panel).

RS_PUP